



A Phloem-Expressed *PECTATE LYASE-LIKE* Gene Promotes Cambium and Xylem Development

Max Bush[‡], Vishmita Sethi^{†‡} and Robert Sablowski*

Cell and Developmental Biology Department, John Innes Centre, Norwich Research Park, Norwich, United Kingdom

OPEN ACCESS

Edited by:

Cristina Ferrandiz,
Polytechnic University of Valencia,
Spain

Reviewed by:

Peter Etchells,
Durham University, United Kingdom
Rosemary White,
Commonwealth Scientific
and Industrial Research Organisation
(CSIRO), Australia

*Correspondence:

Robert Sablowski
robert.sablowski@jic.ac.uk

† Present address:

Vishmita Sethi,
Indian Institute of Science Education
and Research, Kolkata, India

[‡]These authors have contributed
equally to this work

Specialty section:

This article was submitted to
Plant Development and EvoDevo,
a section of the journal
Frontiers in Plant Science

Received: 02 March 2022

Accepted: 17 March 2022

Published: 26 April 2022

Citation:

Bush M, Sethi V and Sablowski R
(2022) A Phloem-Expressed
PECTATE LYASE-LIKE Gene
Promotes Cambium and Xylem
Development.
Front. Plant Sci. 13:888201.
doi: 10.3389/fpls.2022.888201

The plant vasculature plays essential roles in the transport of water and nutrients and is composed of xylem and phloem, both of which originate from undifferentiated cells found in the cambium. Development of the different vascular tissues is coordinated by hormonal and peptide signals and culminates in extensive cell wall modifications. Pectins are key cell wall components that are modified during cell growth and differentiation, and pectin fragments function as signals in defence and cell wall integrity pathways, although their role as developmental signals remains tentative. Here, we show that the pectin lyase-like gene *PLL12* is required for growth of the vascular bundles in the Arabidopsis inflorescence stem. Although *PLL12* was expressed primarily in the phloem, it also affected cambium and xylem growth. Surprisingly, *PLL12* overexpression induced ectopic cambium and xylem differentiation in the inflorescence apex and inhibited development of the leaf vasculature. Our results raise the possibility that a cell wall-derived signal produced by *PLL12* in the phloem regulates cambium and xylem development.

Keywords: Arabidopsis, shoot development, pectate lyase, phloem, cambium, xylem

INTRODUCTION

The vasculature of land plants is critical for growth, as it distributes water and nutrients throughout the plant and provides mechanical support (Ruonala et al., 2017). Each vascular bundle contains three types of tissues: xylem, including water-transporting xylem elements, the mechanically reinforced xylem fibres and parenchyma; phloem, containing the sugar-transporting sieve elements, the companion cells that regulate movement of molecules in and out of the phloem, phloem fibres and parenchyma; and cambium, a layer of undifferentiated cells that produces new xylem cells toward the plant's main axis and new phloem cells away from it (Nieminen et al., 2015).

During the early stages of vascular development, the position of xylem, phloem and the procambium (precursor of the cambium) is defined by intercellular signals mediated by the auxin and cytokinin hormones, in combination with mobile transcription factors and microRNAs (Carlsbecker et al., 2010; Miyashima et al., 2019). The subsequent production of new vascular cells by the cambium is regulated by the peptide signals CLAVATA3/EMBRYO SURROUNDING REGION (CLE) CLE41/CLE44, which activate the Phloem Intercalated With Xylem (PXY) receptor to regulate the balance between the production of new phloem and xylem cells (Ito et al., 2006; Fisher and Turner, 2007; Hirakawa et al., 2008). The ensuing differentiation of these tissues is guided by cell type-specific transcription factors, such as *VASCULAR-RELATED NAC DOMAIN 6*

(*VND6*) and *VND7*, which specify xylem cell types (Kubo et al., 2005), or Altered Phloem Development (APL) (Bonke et al., 2003) and *NAC DOMAIN-CONTAINING PROTEIN 45* (*NAC45*) (Furuta et al., 2014), which control phloem differentiation.

Among the processes regulated during vascular differentiation, modifications of the cell wall feature prominently, for example in the deposition of lignified hoops that mechanically reinforce xylem elements (Mitsuda et al., 2007; Sugiyama et al., 2017), or in the development of perforated plates that connect adjacent sieve elements (Kalmbach and Helariutta, 2019). Pectic polysaccharides, of which the most abundant form is homogalacturonan, are important components of the plant cell wall that are modified during cell growth and differentiation. Pectins are secreted in a methyl-esterified form and modified by pectin methyl-esterase (PME) to control the degree of methylesterification. Pectins with low levels of methylesterification bind Ca^{2+} within the cell wall to form a cross-linked gel that surrounds cellulose and is believed to decrease cell wall extensibility (Wolf et al., 2012; Yang et al., 2018). Developmentally controlled pectin methylesterification modulates not only wall extensibility, but also access to further cell wall-modifying enzymes, such as those involved in the deposition of lignin during xylem differentiation (Wolf et al., 2012).

One group of cell wall modifiers that target demethylesterified pectin are the PECTATE LYASE-LIKE (PLL) proteins, which are found throughout the plant kingdom and are encoded by large gene families (Ulusik and Seymour, 2020). PLLs have an N-terminal signal peptide that targets them for secretion into the cell wall, where they cut homogalacturonan at $\beta(1-4)$ linkages to generate oligogalacturonides (OGs) of different sizes (Sénéchal et al., 2014; Yang et al., 2018). Pectin cleavage occurs during cell expansion or remodelling, and in the middle lamella during cell separation (Yang et al., 2018). Accordingly, PLLs have been implicated in cell expansion processes, such as elongation of cotton fibres (Sun et al., 2020), in secondary wall formation in the xylem, and in cell separation during fruit ripening (Ulusik and Seymour, 2020). Additionally, the OGs produced during pectin cleavage have a signalling role, studied mostly in relation to pathogen attack and as part of the cell wall integrity pathway (Brutus et al., 2010; Ferrari et al., 2013). Externally applied OGs also have developmental consequences, for example by inhibiting the effect of auxin on pea stem elongation (Branca et al., 1988), although a role for OGs as endogenous developmental signals still remains to be established (Ferrari et al., 2013).

Here, we characterise the function of *PLL12* in *Arabidopsis* vascular development. We selected this gene based on ChIP-seq data for the BEL1-like homeodomain transcription factor REPLUMLESS (RPL) (also known as PENNYWISE, PNY and BELLRINGER, BLR) (Byrne et al., 2003; Roeder et al., 2003; Smith and Hake, 2003), which is required for correct vascular patterning (Smith and Hake, 2003; Etchells et al., 2012) and directly interacts with multiple genes that regulate vascular development, such as *PXY*, *CLE41* and *NAC45* (Bencivenga et al., 2016). Furthermore, RPL has been implicated in the expression of cell wall enzymes involved in vascular differentiation (Peaucelle et al., 2011; Etchells et al., 2012). We reasoned that

less well-characterised RPL target genes, such as *PLL12*, might reveal novel aspects of vascular development. Our functional analysis showed that *PLL12* is expressed in the phloem but has unexpected cell non-autonomous effects on cambium and xylem development.

MATERIALS AND METHODS

Plant Material

Plants were grown on JIC *Arabidopsis* Soil Mix (Levington F2 compost plus Intercept and 4 mm grit at a 6:1 ratio) at 16°C under continuous light (100 mE) or in a Sanyo cabinet at 18°C under 16 h light/8 h dark cycles (100 mE). *Arabidopsis thaliana* Columbia (Col) and Landsberg-*erecta* (L-*er*) were used as wild-types; *pll12* (AT5g04310; SAIL 1149_C06) was obtained from The Nottingham Arabidopsis Stock Centre and genotyped using primers 1–3 **Table 1**. For the construction of *RPS5A:LhGR:opPLL12*, the *PLL12* CDS was amplified from Col cDNA (primers 12–13 **Table 1**), cloned into pGEMT-EASY, sequenced, moved into pOWL49 by *Sall/KpnI* restriction cloning and transformed into *RPS5A:LhGR* in L-*er* background. Transformants were selected on gentamycin/kanamycin Murashige and Skoog medium (M&S) with agar, transferred to soil and treated at appropriate developmental stages with either 10 μM dexamethasone (from a 10 mM stock in ethanol) or the equivalent volume of ethanol (mock-treatment) diluted in aqueous 0.015% Silwet L-77 (49). Some seedlings were germinated and grown on M&S agar and then transferred to M&S agar supplemented with either 10 μM dexamethasone or ethanol (mock).

To complement the *pll12* phenotype, a full length *pPLL12:PLL12* construct was generated as follows. Using Columbia genomic DNA and Phusion polymerase (New England Biolabs), the promoter and 5' utr (1,884 bp) were amplified as two fragments, the gene (3,997 bp) as four fragments and the 702 bp 3' utr as a single fragment using primers 14–27 in **Table 1**. The seven fragments were assembled into plasmid G45 by Golden Gate cloning (Engler et al., 2014). The assembly was verified by sequencing and inserted into plasmid G800 by Gateway cloning. For construction of *pPLL12:PLL:GUS*, *PLL12* was amplified from Col-0 genomic DNA and fused in-frame with GUS and cloned into pPZP222 (Hajdukiewicz et al., 1994) using Golden Gate cloning as above, with primers listed in **Table 1**. The final constructs were transformed into Col-0 by the floral dip method (Clough and Bent, 1998) and transformants were selected on Murashige and Skoog medium supplemented with gentamycin 100 $\mu\text{g}/\text{mL}$.

Measurements of Stem Growth

Arabidopsis Col and *pll12* plants were grown until the first flower reached stage 17 (Smyth et al., 1990), ink marks were placed on the stem at 2 mm intervals and photographed next to a ruler using a Nikon D3100 DSLR camera and 18–55 mm VR lens. Plants were returned to the growth cabinet for 4 d and then re-photographed. Manual land marking of the stem ink marks and calibration points on the ruler was performed using the Point Picker plugin

TABLE 1 | Oligonucleotide sequences.

Number	Name	Sequence
Genotyping		
1	PLL12 F	TCATTTTCATGCTTTATCTTGTG
2	PLL12 R	CCTGACTATTAATTGTAGGGCTA
3	SAIL LB1 TDNA	GCCTTTTCAGAAATGGATAAATAGCCTTG CTTC
RT-PCR		
4	PLL12 RTPCR F1	ATGGTGGCTCATGAGAGGAGGATCC
5	PLL12 RTPCR R1	CTATGATCTCGTATGGTGTGGAATATA
6	PLL12 RTPCR R2	CTTTGAACATTAAGAACAACATGTTT
7	PLL12 RTPCR R3	TOGTCGTGACCTAGGAGCATAACC
qPCR		
8	PLL12 qPCR F	TCCCAATGCCAAAGAGGTAACG
9	PLL12 qPCR R	TCCAGTTCCATCCCGACCAATG
10	TUBULIN4 qPCR F	CTGTTTCCGTACCCTCAAGC
11	TUBULIN4 qPCR R	AGGGAACGAAAGACAGCAAG
pOp:PLL12		
12	PLL12 CDS F	<u>CTGTCGACATGGTGGCTCATGAGAGGAGG</u>
13	PLL12 CDS R	<u>CTGGTACCCTATGATCTCGTATGGTGTGG</u>
pPLL12:PLL12		
14	pPLL12 fragment 1 F	<u>GTGGTCTCAGGAGACCTGGTCTGGTTTC</u> ATCAGC
15	pPLL12 fragment 1 R	<u>GTGGTCTCAGAAATCGAATCAATGAAACT</u> CTTG
16	pPLL12 fragment 2 F	<u>GTGGTCTCGTTTCTTTAGTGAAGATACA</u> TTTG
17	pPLL12 fragment 2 R	<u>GTGGTCTCACATTATATCTCTATTATATC</u> TTATG
18	PLL12 gene fragment 1 F	<u>GTGGTCTCTAATGGTGGCTCATGAGA</u> GGAGG
19	PLL12 gene fragment 1 R	<u>GTGGTCTCTGATGAGAGAAATAGT TGTTG</u>
20	PLL12 gene fragment 2 F	<u>GTGGTCTCGCATCACGACGAGGT TATGC</u>
21	PLL12 gene fragment 2 R	<u>GTGGTCTCGGCAATGACCGTGAGC TGGTC</u>
22	PLL12 gene fragment 3 F	<u>GTGGTCTCAATGCCGGCGTTTTCGG CGATC</u>
23	PLL12 gene fragment 3 R	<u>GTGGTCTCACCTTGGCTAAAGAATGCT AAAC</u>
24	PLL12 gene fragment 4 F	<u>GTGGTCTCGCAAGTTGGTATATCTCAA AAAC</u>
25	PLL12 gene fragment 4 R	<u>GTGGTCTCTAAGCCTATGATCTCGTATG</u> GTGTGG
26	PLL12 3'utr F	<u>GTGGTCTCAGCTTTTTCATTATTGGTTCATA</u> GTTAC
27	PLL12 3'utr R	<u>GTGGTCTCAAGCGAAGGGAAATCCTGA</u> ATTGACTTG
PXY RNA in situ hybridisation		
28	PXY F in situ	<u>AAGGATCCATCAGCAATAACCTCTCAGG</u> TGAAG
29	PXY R in situ	<u>AAGTCGACTGCATCCAACGTAATTTGGGA</u> TTTCAC

Sequences re shown in 5'–3' orientation. Restriction enzyme sites are underlined, Golden Gate recombination overhangs are shown in italics.

of Fiji (Schindelin et al., 2012). Digitalised coordinates were measured, graphs were plotted, and Mann-Whitney U tests and Student's t tests were performed using standard functions in matplotlib,¹ Python 2.7, and Scientific Python.²

Microscopy and Staining

Expression of GUS reporters in stem tissue was performed as described (Sieburth et al., 1998), stained tissue was observed with a Leica S8APO stereozoom or Zeiss Axio Imager Z2.

¹<http://matplotlib.org>

²<http://www.scipy.org>

Modified pseudo-Schiff propidium iodide (mPS-PI) staining was performed before imaging samples with a Zeiss LSM780 confocal microscope as described (Serrano-Mislata et al., 2015). Staining with 0.04% Calcofluor was performed on Technovit sections for 5 min at room temperature.

To determine if xylem bundles in *pll12* stems were continuous and intact, 1 cm stem apices were stained with propidium iodide (Banasiak et al., 2019) and examined using a Zeiss Axiozoom V16 microscope.

Tissues for light microscopy were fixed in either 1% glutaraldehyde in 0.05 M cacodylate buffer pH 7.2 or formalin:acetic acid:ethanol (4:5:50), dehydrated in an ethanol series and embedded in Technovit following the manufacturer's instruction. Sections were cut 5 μm thick with glass knives and a Leica ultramicrotome UC7, stained with toluidine blue and examined with a Zeiss Axio Imager Z2 microscope.

Stems for vibratome sectioning were prepared following the protocol of Wang et al. (2014), sections were cut 25–30 μm thick using a Leica VT1000S vibratome, stained with phloroglucinol-HCl (Mitra and Loqué, 2014) and mounted on glass slides following Speer's modification (Speer, 1987).

RNA in situ Hybridisation Experiments

Stem apices of *RPS5A:LhGR:opPLL12* plants were treated with or without dexamethasone: all stem apices were fixed and subsequently processed according to Rebocho et al. (2017). Serial sections from control (mock-treated) and experimental (dex-treated) samples were collected onto the same Poly-L-Lysine coated slide. Duplicate slides were sandwiched together between plastic spacers and loaded with either sense or antisense probes. To generate specific digoxigenin-labelled riboprobes probes, 550 bp of PXY coding sequence was cloned using primers 28–29 (Table 1) and BamH1/SalI ligated into pBluescript II KS9 (±). Antisense probes were PCR amplified using combinations of M13R primer and the specific gene F primer, whilst sense probes were amplified similarly using M13F and specific gene R primers. Purified antisense and sense probes were obtained by RNA transcription using the T3 and T7 promoters respectively following the protocol of Rebocho et al. (2017).

Rhodamine B Uptake

Col and *pll12* plants grown to the same developmental stage (3–5 flowers/siliques) were removed from their pots and very gently washed under running tap water to remove soil from the root balls before blotting dry with absorbent paper towels. Roots were then threaded through holes cut into a disc of polystyrene foam and the plants floated in a glass beaker containing 50 ml of 0.25% rhodamine B (w/v) so that the roots were immersed in the solution. Batches of 3–4 Col and *pll12* plants were incubated simultaneously under a 6 h light-8 h dark-6 h light regime at 16°C in a Sanyo cabinet. The following day, excess dye was rinsed off the roots which were then blotted dry and the plants photographed and stem samples collected. All but the smallest flower buds were removed before the apical 1 cm and basal 1 cm of stem above the rosette were isolated, frozen in liquid nitrogen and stored at –70°C. Individual stem samples were ground up in 400 μl protein extraction buffer (100 mM HEPES pH 7.5, 5% v/v

glycerol, 50 mM KCl, 5 mM EDTA, 0.1% v/v Triton X-100, 1 mM DTT and one Complete EDTA-free protease inhibitor cocktail tablet/50 ml buffer) and rotated at 4°C for 1 h to extract soluble proteins and the rhodamine B dye. After a 10 min centrifugation at 12,000 g to pellet insoluble material, 100 μ l aliquots of the extracts were collected into wells of a 96-well microtitre plate and assayed spectrophotometrically at $A_{550\text{nm}}$; dye concentrations were calculated against a rhodamine B standard curve. Soluble proteins were isolated from the extracts by methanol-chloroform precipitation and the rhodamine B removed by methanol washes, protein pellets were then resuspended in 100 μ l of protein extraction buffer and protein concentrations calculated by Bradford reactions.

Quantitative Reverse Transcription-Polymerase Chain Reaction

mRNA levels were measured by quantitative reverse transcription-polymerase chain reaction (qRT-PCR) as published (Schiessl et al., 2012), with primers 8–11 listed in **Table 1**.

RESULTS

Genes annotated as belonging to the pectin lyase superfamily are enriched among candidate targets of RPL (Bencivenga et al., 2016; **Supplementary Table 1**); among these, *PLL12* (*AT5G04310*) showed clear binding to RPL in three ChIP-seq biological replicates, but in none of the negative controls

(**Supplementary Figure 1**). Furthermore, *PLL12* expression was located specifically in vascular cell types in a root transcriptomic atlas (Brady et al., 2007) and was associated with vascular differentiation *in vitro* (Kondo et al., 2016). Based on these data, we hypothesised that *PLL12* might have a role in cell wall modification during vascular development, in addition to the previously described function in stomatal guard cells (Chen et al., 2021).

To confirm the *PLL12* expression during vascular development, we used the GUS reporter fused to the complete *PLL12* gene. Previous reporter genes using GUS fused to 2 kb of the putative *PLL12* promoter gave weak and variable expression (Sun and Van Nocker, 2010) or suggested widespread expression (Chen et al., 2021). Our ChIP-seq data, however, indicated RPL binding to intron 3 of *PLL12* (**Supplementary Figure 1**), raising the possibility that regulatory sequences have been missed in previous constructs. To include all potential regulatory sequences, we used a genomic fragment that fully complemented the *pll12* mutation (see below), with GUS fused in frame after the last exon of *PLL12*. In nine independent lines, this *pPLL12:PLL12-GUS* reporter was expressed in stomata and throughout the vasculature of seedlings (**Figure 1**). In both the root and in the inflorescence, expression initiated close to the apical meristem, indicating that *PLL12* begins to function during early stages of vascular development. Cross-sections of the stem showed that within the vascular strands, *PLL12* was expressed primarily in the phloem. This localised expression pattern was in agreement with the reported role of *PLL12* in stomatal guard cells (Chen et al., 2021) and with reports of phloem-specific

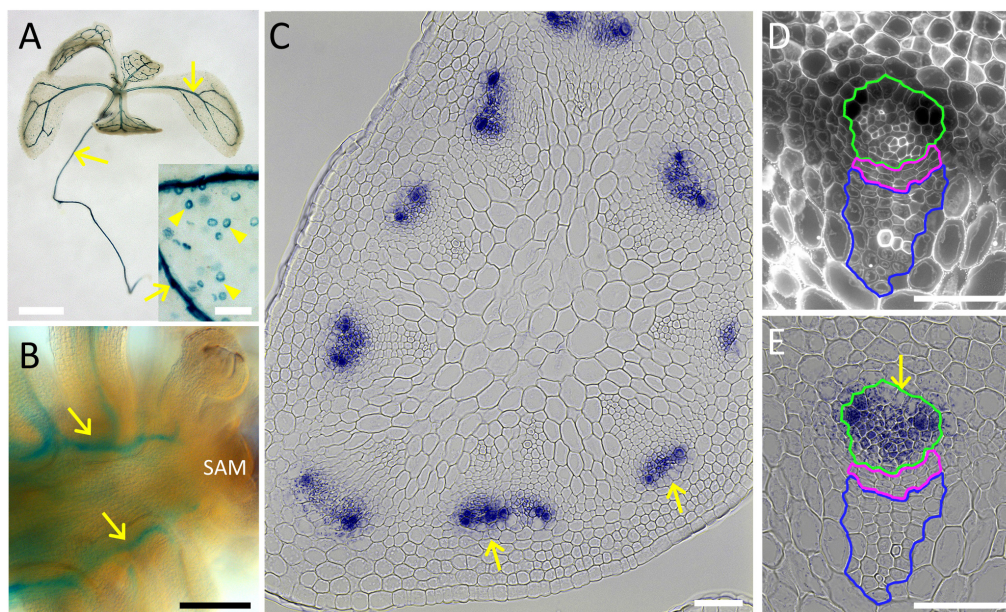


FIGURE 1 | *PLL12* is expressed in the stem phloem. **(A,B)**: *pPLL12:PLL12:GUS* seedling **(A)** and inflorescence apex **(B)** stained for GUS and cleared with chloral hydrate, showing GUS activity in the vasculature (arrows); in panel **(A)**, note also the dotted signal on cotyledons due to expression in stomatal guard cells. Bars: 1 cm **(A)**, 500 μ m **(B)**. **(C–E)**: Cross-section of the inflorescence stem showing *pPLL12:PLL12:GUS* expression in phloem cells; **(C)**: overview of a stem section, with GUS staining in part of the vascular bundles (arrows); **(D)**: calcofluor-stained section through a single vascular bundle, with the phloem, cambium and xylem regions enclosed in green, magenta, and blue lines, respectively; **(E)**: same section as in panel **(D)**, showing GUS staining specifically in the phloem (arrow); bars: 50 μ m.

PLL12 expression in the root (Brady et al., 2007; Kalmbach et al., 2022) and during *in vitro* differentiation (Kondo et al., 2016).

We next analysed the function of *PLL12*, focussing especially on vascular development. For this, we used two independent T-DNA mutant alleles, *pll12-1* (SAIL 1207_A07) (Chen et al., 2021) and *pll12-2* (SAIL 1149_C06). As reported, *pll12-1* had undetectable *PLL12* mRNA (Chen et al., 2021), and the same was seen for *pll12-2* (Supplementary Figure 2). Both alleles caused similar phenotypes: the mutants were dwarf and late flowering, with slow stem growth (Figure 2). Complementation with full genomic fragments (from 1,884 bp upstream of the start codon to 702 bp downstream of the stop codon) confirmed that the *pll12* mutations caused these phenotypes, and that the selected genomic region contained all regulatory and coding regions required for function (Figure 2). Because the mutants had comparable and fully recessive phenotypes, from this point on we used the previously characterised *pll12-1* mutant.

The vascular pattern of *pll12-1* appeared normal and was uninterrupted in leaves and in the inflorescence apex

(Supplementary Figure 3). The vascular bundles contained all the expected cell types in their correct positions, but appeared smaller, especially in the mature region of the inflorescence stem (Figure 3). To detect growth defects, we measured the size and cell numbers in different regions of the stem vasculature. To compensate for differences in the growth rate between the mutants and the wild type, stems were collected when the fifth flower had matured (i.e., after a longer period of growth in *pll12-1*). Within stems at this stage, we collected sections at two positions: at the base of the fifth flower, corresponding to the immature region of the stem, which is still elongating (less than 1 cm of the apex, see Figure 2), and near the first silique, where stem elongation is complete and the vascular bundles have started to deposit secondary cell walls (more than 2 cm from the apex, Figure 2). In *pll12-1*, the size of immature vascular strands was not different from the wild type (number of cells per cross-section, mean \pm SD: 101.4 \pm 19.9 in wt, 98.7 \pm 15.9 in *pll12-1*, Supplementary Table 2). However, as the stem matured, differences became clearer (213.9 \pm 27.7 in wt, 142.4 \pm 33.5 in *pll12-1*, Supplementary Table 2) and, contrary to the expectation based on the expression pattern, were not specific to the phloem. Instead, all three regions of the vascular strand (phloem, cambium and xylem) had reduced growth, measured either by cross-sectional area or cell numbers (Figures 3D,F-H). The region most affected was the cambium, which already had significantly fewer cells in the mutant before differences were detectable in the phloem and xylem (Figures 3G,H). Furthermore, the cambium was the only region with no detectable growth (measured as either cross-sectional area or by number of cells in cross-section), in contrast to the phloem and xylem, which grew at about half the wild-type rate. These results showed that *PLL12* is not essential for the initial vascular patterning or differentiation but is required for subsequent growth of all regions of the vascular strand, particularly the cambium.

To reveal physiological consequences of the histological defects described above, we investigated whether *pll12-1* affected phloem and xylem function. Using carboxyfluorescein diacetate (CFDA) as a tracer, reduced phloem transport from hypocotyls to roots was shown in *pll12* seedlings (Kalmbach et al., 2022). Although we were not able to adapt this method to measure phloem transport in the inflorescence stem, it would be reasonable to assume that a similar defect would occur in the stem vasculature. As an indirect method to detect defects in phloem function in the stem, we assayed for high starch levels after a dark period, which are typically seen in plants with compromised sugar transport (Barratt et al., 2010; Bezruczyk et al., 2018). Consistent with a defect in sugar export, staining with Lugol's Iodine reagent revealed a strong accumulation of starch in the cortex of the inflorescence stem in *pll12-1* compared to the wild type (Figure 4). To assess xylem function, we measured transport of rhodamine B dye from roots to the inflorescence apex. Both visually (Figures 4E,F) and based on the dye concentration in the apex (normalised to protein concentration, Figure 4G), the mutant showed a clear reduction in transport through the xylem. We conclude that the reduced growth of vascular bundles in *pll12* was accompanied by a decrease in both sugar and water transport,

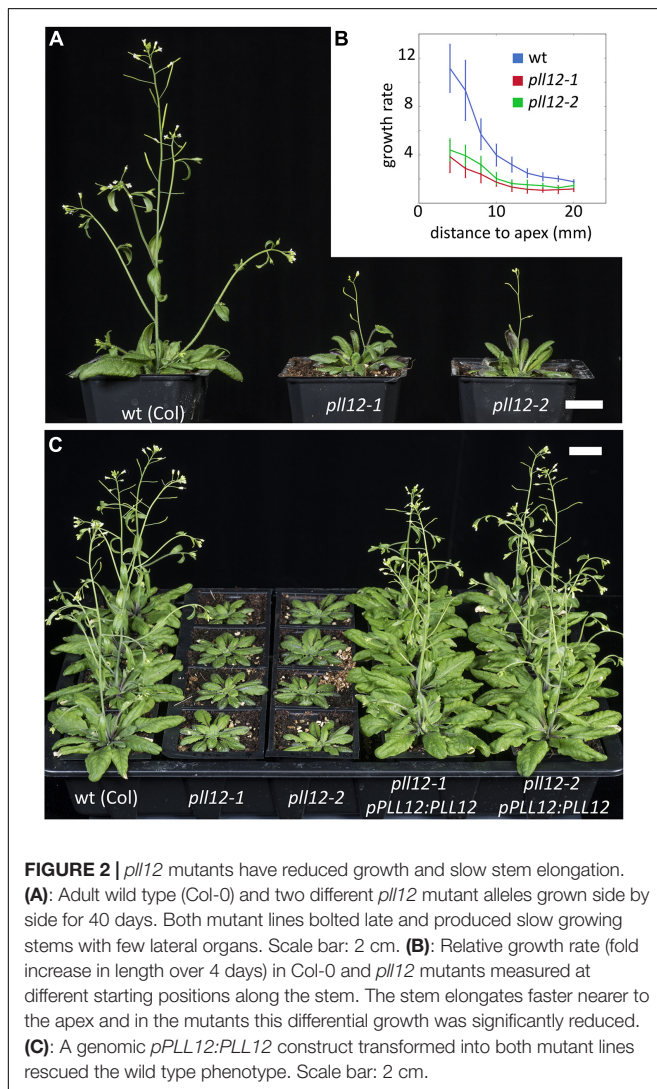
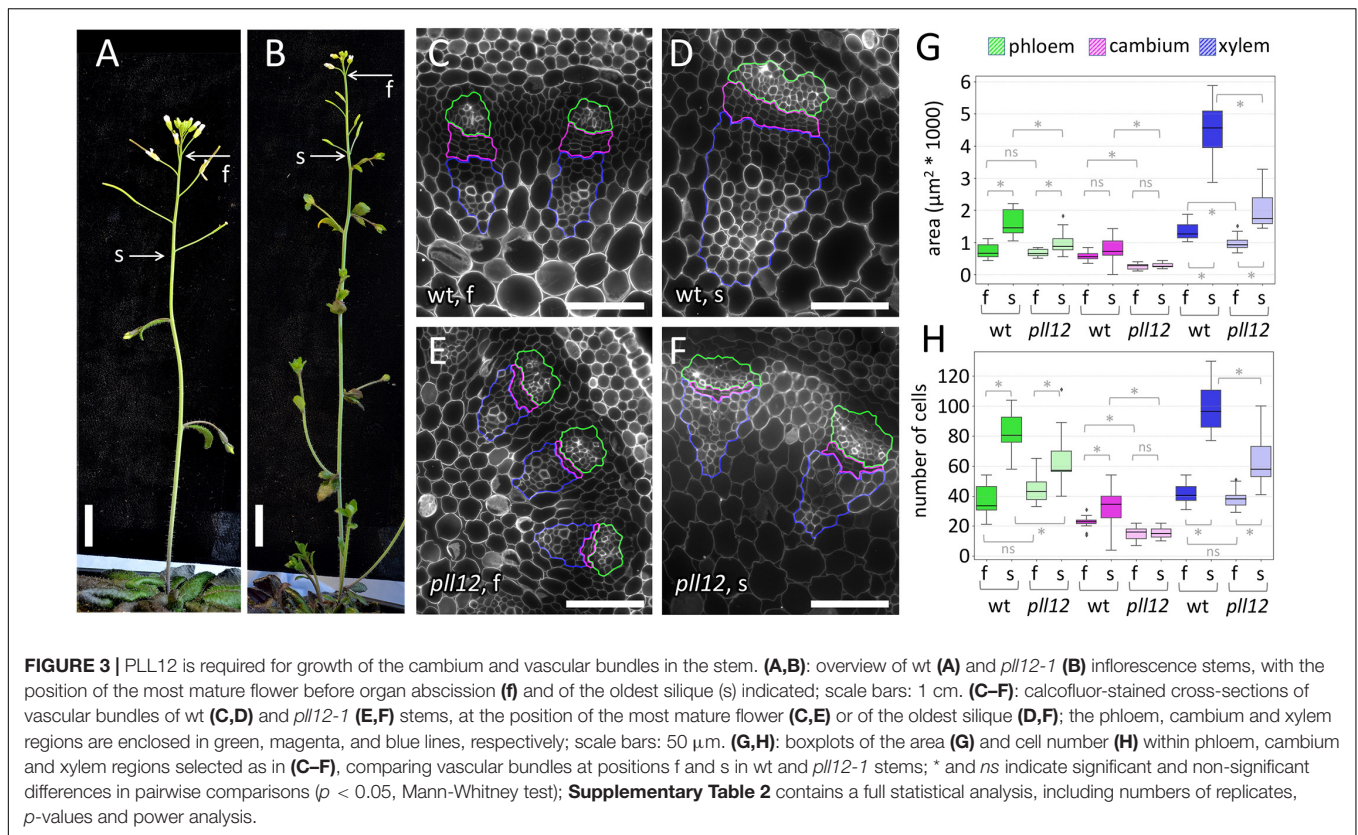


FIGURE 2 | *pll12* mutants have reduced growth and slow stem elongation. (A): Adult wild type (Col-0) and two different *pll12* mutant alleles grown side by side for 40 days. Both mutant lines bolted late and produced slow growing stems with few lateral organs. Scale bar: 2 cm. (B): Relative growth rate (fold increase in length over 4 days) in Col-0 and *pll12* mutants measured at different starting positions along the stem. The stem elongates faster nearer to the apex and in the mutants this differential growth was significantly reduced. (C): A genomic *pPLL12:PLL12* construct transformed into both mutant lines rescued the wild type phenotype. Scale bar: 2 cm.



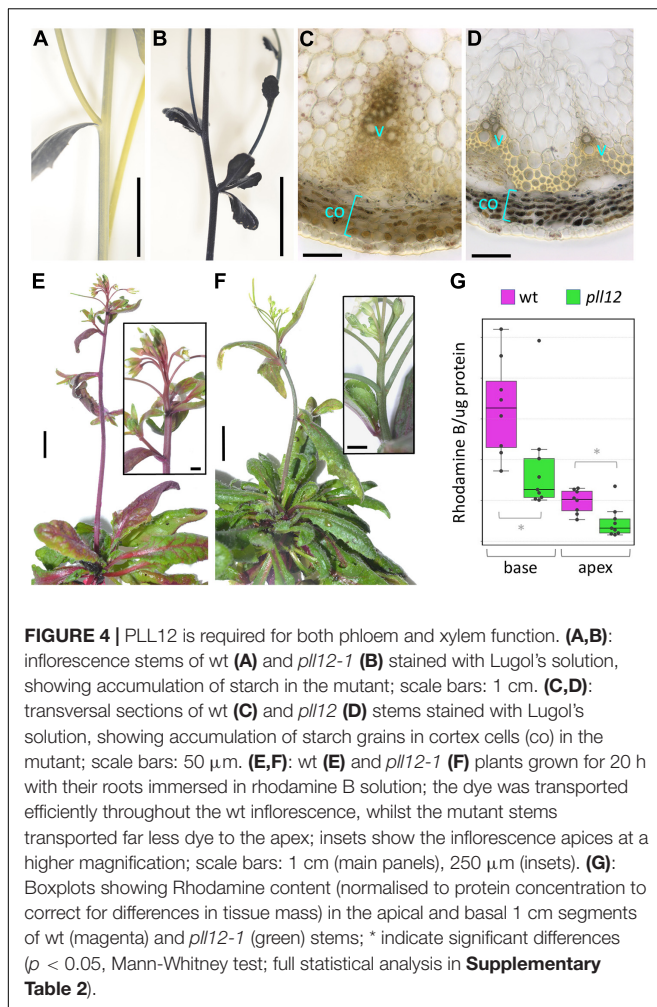
which might be the cause of the general inhibition of growth in the mutant. Similarly, slow growth of the cambium and xylem in the mutant might be an indirect consequence of a reduced sugar supply, caused by a primary defect in the phloem. Alternatively, *PLL12* might be required to produce a phloem-derived signal that promotes development of the cambium and xylem.

To test whether increased or ectopic *PLL12* expression might be sufficient to promote cambium and xylem development, we generated plants in which *PLL12* transcription could be induced ubiquitously. To do this, we used a *pOp:PLL12* construct expressed in an *RPS5A:LhGR* background; when tissues are exposed to dexamethasone, this system induces *PLL12* expression under the widely expressed *RIBOSOMAL SUBUNIT 5A* promoter (**Supplementary Figure 4**). After inflorescence tips were treated five times at 2-day intervals, dexamethasone-treated plants showed variable inhibition of growth, ranging from short internodes to death of the shoot apex (**Figures 5A–C**). These phenotypes were associated with different levels of lignin deposition in the cortex and vascular bundles within 1–2 mm below the shoot meristem (**Figures 5D–F**). In apices with a mild phenotype, it was possible to trace the earliest deposition of ectopic lignin to strands of cells leading basally away from the shoot apical meristem—this position is typically occupied by procambial strands in the wild type (**Supplementary Figure 5**), suggesting that cells at early stages of vascular differentiation were particularly sensitive to ectopic *PLL12* expression.

Ectopic lignification is one of the responses elicited by cell wall fragments during pathogen attack (Ferrari et al., 2013),

so lignification could have been a defence response activated by pectin fragments produced when *PLL12* was overexpressed. However, closer examination of the dexamethasone-treated apices revealed cortex cells with lignification in a pitted pattern and openings between adjacent cells (**Figure 5I**), similar to root metaxylem and to ectopic metaxylem cells induced by the regulators of xylem differentiation, *VND6* and *SND5* (**Figures 5G–I**; Kubo et al., 2005; Zhong et al., 2021). Pitted cells were also seen within the vascular bundles of plants with a mild phenotype after *PLL12* induction, but not in uninduced controls (**Supplementary Figure 5**). Further supporting the idea that ectopic *PLL12* expression re-directed cortex cells to vascular development, ectopic expression of the regulator of cambium development, *PXY*, was detected by *in situ* hybridisation after *PLL12* induction (**Figure 5N**). Conversely, the normal *PXY* expression in the cambium of the wild type was disrupted in the disorganised vascular bundles seen after dexamethasone treatment (**Figures 5J–O**). Together with the inhibition of cambium and xylem growth in the *pll12-1* mutant (**Figure 3**), the results above supported a role for *PLL12* in the regulation of cambium and xylem development, although the experiments could not distinguish whether *PLL12* promoted cambium and xylem identity sequentially, or separately in different cells.

The stronger effects of *PLL12* overexpression close to the meristem and in cortex cells suggested that the response to a putative *PLL12*-produced signal depended on developmental stage and cell type. To study the effect of ectopic *PLL12* in a different context, we also looked at seedlings.



RPS5A:LhGR pOp:PLL12 plants were grown on medium without dexamethasone until the first pair of leaves emerged, then the seedlings were moved on to dexamethasone or mock treatment plates. Over the subsequent 7 days, a gradient of phenotypes became evident, ranging from small rosettes to stunted seedlings with severely deformed leaves (**Figure 6**), although root growth was initially unaffected (**Supplementary Figure 6**). In the most extreme cases, leaf blades failed to expand and became chlorotic (**Figures 6D,E**). Confocal imaging of these leaves stained with mPS-PI showed that the veins had irregular thickness, were discontinuous and showed cambium-like cell divisions along the leaf vasculature (**Figures 6F–L**). Thus, although ectopic *PLL12* only appeared to induce extensive lignification in the inflorescence apex, it interfered with the differentiation of vascular cells both in the inflorescence and in seedlings.

DISCUSSION

PLL12 has been shown to function in stomatal guard cells, where it affects cell wall properties and the speed of stomatal opening and closure (Chen et al., 2021). Here, we show that *PLL12* is

also required for the development and function of the stem vasculature. Loss of *PLL12* function did not have obvious effects on patterning or cell differentiation, but inhibited growth of vascular bundles, with the earliest effects visible in the fascicular cambium, followed by reduced cell numbers in both phloem and xylem. The reduced cell numbers throughout the stem vascular bundles were accompanied by reduced transport of both water and sugar. The simplest interpretation of these phenotypes is that *PLL12* function is limiting for the activity of the fascicular cambium, and consequently for the enlargement of vascular bundles during stem growth.

Despite the reduced growth across the vasculature (**Figures 3G,H** and **Supplementary Table 2**), *PLL12* expression was specific to the phloem, in line with previous reports (Brady et al., 2007; Kalmbach et al., 2022). Thus, the effects on cambium and xylem growth were likely indirect consequences of a primary role of *PLL12* in the phloem. In support of a phloem function for *PLL12*, a recent pre-print reports that *pll12-1* has a defect in long-distance phloem transport, attributed to subtle changes in the formation of sieve plates between phloem elements (Kalmbach et al., 2022). However, defects in long-distance sugar transport would not readily account for the disproportionate effect of *pll12-1* on the growth of established vascular bundles, in comparison to earlier stages. Moreover, a role exclusively in sieve plate formation would not easily explain why *PLL12* overexpression induced ectopic cambium and xylem features and disrupted vascular differentiation in seedlings. To explain both loss- and gain-of-function phenotypes, and taking into account the phloem-specific expression, we propose that in addition to the reported role in sieve element development (Kalmbach et al., 2022), *PLL12* activity influences an intercellular signal that coordinates development across vascular tissues.

PLL12 contains a canonical pectate lyase C domain, with conserved residues implicated in catalysis, Ca^{++} binding and exocytosis (Chen et al., 2021), so this protein is likely to cleave demethylesterified pectin within the cell wall. Accordingly, immunolocalisation showed increased levels of calcium-crosslinked pectin in *pll12-1* stomatal walls (Chen et al., 2021) and mutation of the predicted pectate lyase catalytic site abolished the ability of *PLL12* to complement the mutant (Kalmbach et al., 2022). Furthermore, *PLL12* is homologous to a *Zinnia* PLL protein for which pectate lyase activity has been demonstrated *in vitro* (Domingo et al., 1998). Pectin cleavage would be expected to release oligogalacturonides (OGs), which bind to the WAK1 receptor and activate the cell wall integrity and pathogen defence signalling pathways, whose downstream responses include lignification (Caño-Delgado et al., 2003; Brutus et al., 2010; Ferrari et al., 2013). However, the induction of metaxylem-like pitted cell walls, combined with ectopic *PXY* expression, suggested that lignification after ectopic *PLL12* expression was an aspect of vascular differentiation, rather than a generic defence or cell wall stress response.

Thus, the expected biochemical function of *PLL12*, together with its non-cell-autonomous effects and its ability to ectopically induce cambium and xylem identity, raise the possibility that a cell wall-derived signal participates in the regulation of vascular differentiation. The most straightforward candidate

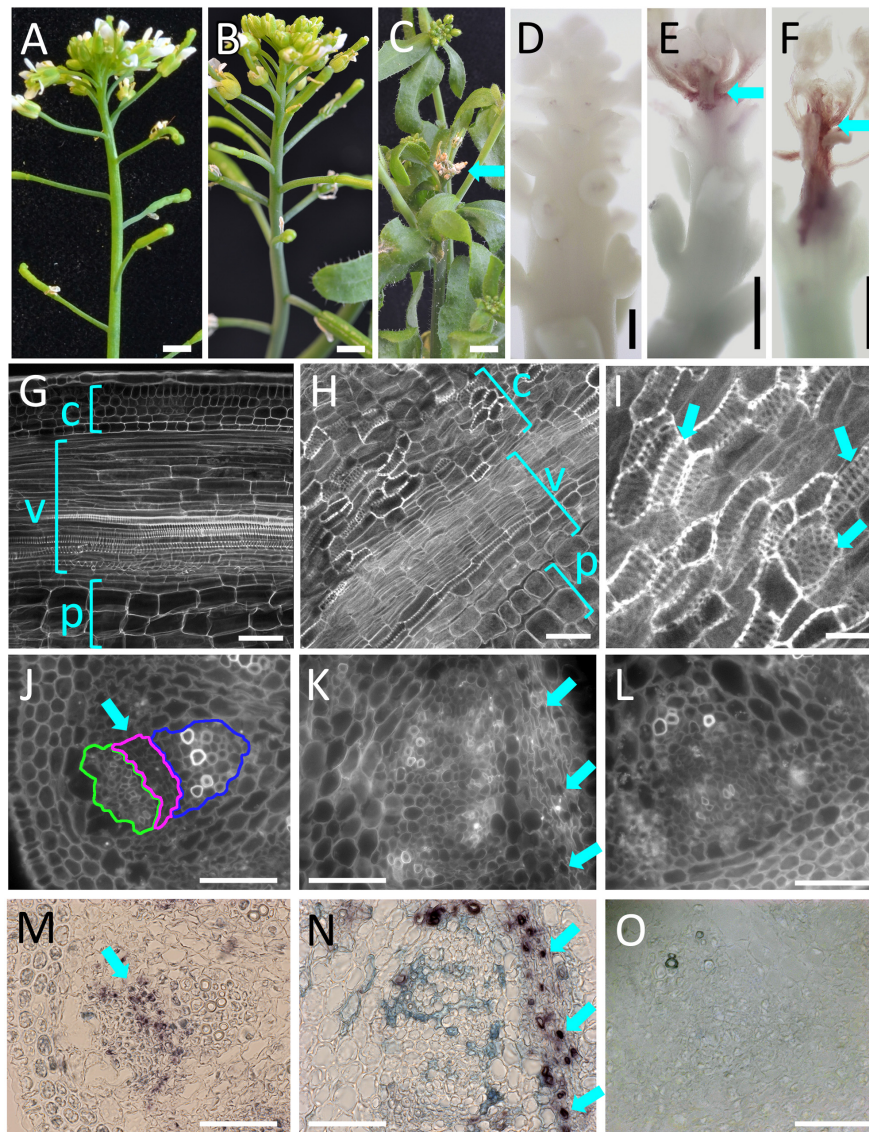


FIGURE 5 | *PLL12* over-expression induces ectopic xylem differentiation and expression of a cambium marker. **(A–C)**: Mock-treated *RPS5A:LhGR;pOp:PLL12* **(A)** looked normal, whilst induction of *PLL12* expression with dexamethasone resulted in mild **(B)**, [shortened internodes] to severe effects **(C)**, [with death of the stem apex (arrow) and lateral organs]; scale bars: 2 mm. **(D–F)**: Mock-treated **(D)** or dexamethasone-treated **(E,F)** inflorescence apices of *RPS5A:LhGR, pOp:PLL12* plants stained with phloroglucinol, showing mild **(E)** to severe **(F)** lignification; scale bars: 400 μm . **(G–I)**: Confocal images of *RPS5A:LhGR:PLL12* stem apices stained with mPS-PI after mock-treatment **(G)** or dexamethasone treatment **(H,I)**; c, v, and p indicate cortex, vasculature and pith; **(I)** higher magnification of stem section similar to panels **(H)**, with arrows indicating cells with the pitted walls characteristic of xylem elements and the top left arrow marking an opening between adjacent pitted cells. Scale bars: 50 μm **(G,H)**, 20 μm **(I)**. **(J–O)**: *In situ* hybridisation experiments showing *PXY* expression after mock **(J,L,M,O)** or dex-treatment **(K,N)** of *RPS5A:LhGR:PLL12* stem apices. All sections were incubated with *PXY* anti-sense probe except **(L,O)** (sense probe controls). **(J–L)** calcofluor images of the corresponding images shown in panels **(M–O)** respectively; in panel **(J)**, phloem, cambium and xylem regions are enclosed in green, magenta and blue lines, respectively. The normal *PXY* expression pattern in the cambial and early xylem precursor cells [arrows in panels **(J,M)**] is disrupted after dexamethasone treatment, which also induces strong *PXY* expression in a subset of cortical cells [arrows in panels **(K,N)**]. Bars: 50 μm .

signal would be OGs, although their developmental roles remain speculative (Seifert and Blaukopf, 2010). Supporting a link to xylem differentiation, genes that respond early to OG treatment (Moscatiello et al., 2006) included *SND5*, which is part of the transcriptional network controlled by *PXY* (Smit et al., 2020) and encodes a NAC domain protein that regulates secondary wall deposition in the xylem (Zhong et al., 2021). However, indirect

effects on other signalling pathways are also possible. External application of OGs has been shown to interfere with auxin signalling (Branca et al., 1988; Ferrari et al., 2013). However, the phenotypes caused by ectopic *PLL12* activation were different from those seen in plants with an overall inhibition of auxin signalling; for example, there was little effect on roots, where auxin plays a central role (Israeli et al., 2020). The interrupted

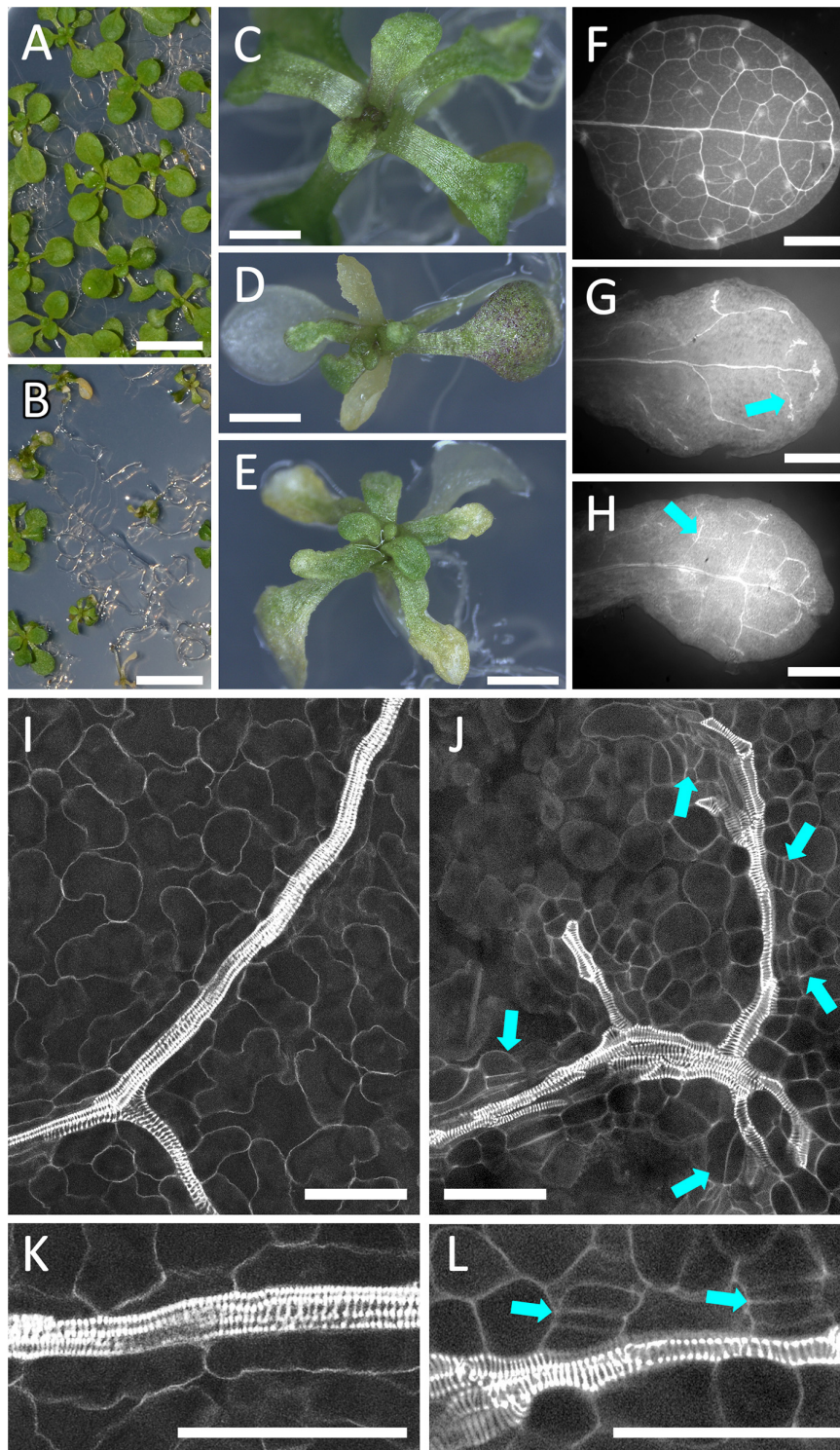


FIGURE 6 | Over-expression of *PLL12* disrupts the development of leaf vasculature. **(A–E)**: *pRPS5A:LhGR pOp:PLL12* plants growing for 4 days on medium containing dexamethasone **(B,D,E)** showed reduced growth and leaf chlorosis, in contrast to mock-treated plants **(A,C)**; scale bars: 5 mm **(A,B)**, 2 mm **(C–E)**. **(F–H)**: Low magnification images of mPS-PI-stained leaves from an uninduced control **(F)** and two seedlings grown for 4 days on dexamethasone-containing medium **(G,H)**; arrows indicate interrupted, uneven vasculature seen after *PLL12* induction; scale bars: 200 μm. **(I–L)**: Confocal images of leaf veins from seedlings comparable to panels **(A–H)**, grown without **(I,K)** or with dexamethasone **(J,L)**; panels **(K,L)** are higher magnifications of panels **(I,J)**; arrows indicate cell divisions oriented parallel to the veins, in a cambium-like pattern; scale bars: 50 μm.

veins seen after ectopic PLL12 induction in cotyledons and leaves are also reminiscent of phenotypes seen after application or overexpression of the PXY ligand CLE41/44 (Hirakawa et al., 2008), or in mutants that affect phosphoinositide-regulated vesicle traffic, which may regulate auxin transport (Sieburth et al., 2006; Carland and Nelson, 2009). In the future, it will be interesting to explore how PLL12 function interacts with these signalling pathways.

DATA AVAILABILITY STATEMENT

The original contributions presented in the study are included in the article/**Supplementary Material**, further inquiries can be directed to the corresponding author.

AUTHOR CONTRIBUTIONS

RS: conceptualisation, software, funding acquisition, and supervision. MB and VS: investigation. MB and RS:

REFERENCES

- Banasiak, A., Biedroń, M., Dolzblasz, A., and Berezowski, M. A. (2019). Ontogenetic changes in auxin biosynthesis and distribution determine the organogenic activity of the shoot apical meristem in pin1 mutants. *Internat. J. Mole. Sci.* 20:180. doi: 10.3390/ijms20010180
- Barratt, D. H. P., Kölling, K., Graf, A., Pike, M., Calder, G., Findlay, K., et al. (2010). Callose Synthase GSL7 Is Necessary for Normal Phloem Transport and Inflorescence Growth in Arabidopsis. *Plant Physiol.* 155, 328–341. doi: 10.1104/pp.110.166330
- Bencivenga, S., Serrano-Mislata, A., Bush, M., Fox, S., and Sablowski, R. (2016). Control of Oriented Tissue Growth through Repression of Organ Boundary Genes Promotes Stem Morphogenesis. *Dev. Cell* 39, 198–208. doi: 10.1016/j.devcel.2016.08.013
- Bezruczyk, M., Hartwig, T., Horschman, M., Char, S. N., Yang, J., Yang, B., et al. (2018). Impaired phloem loading in zmsweet13a, b, c sucrose transporter triple knock-out mutants in *Zea mays*. *New Phytol.* 218, 594–603. doi: 10.1111/nph.15021
- Bonke, M., Thitamadee, S., Mähönen, A. P., Hauser, M.-T., and Helariutta, Y. (2003). APL regulates vascular tissue identity in Arabidopsis. *Nature* 426, 181–186. doi: 10.1038/nature02100
- Brady, S. M., Orlando, D. A., Lee, J.-Y., Wang, J. Y., Koch, J., Dinneny, J. R., et al. (2007). A high-resolution root spatiotemporal map reveals dominant expression patterns. *Science* 318, 801–806. doi: 10.1126/science.1146265
- Branca, C., Lorenzo, G. D., and Cervone, F. (1988). Competitive inhibition of the auxin-induced elongation by α -D-oligogalacturonides in pea stem segments. *Physiol. Plant.* 72, 499–504. doi: 10.1111/j.1399-3054.1988.tb09157.x
- Brutus, A., Sicilia, F., Maccone, A., Cervone, F., and De Lorenzo, G. (2010). A domain swap approach reveals a role of the plant wall-associated kinase 1 (WAK1) as a receptor of oligogalacturonides. *Proc. Natl. Acad. Sci.* 107, 9452–9457. doi: 10.1073/pnas.1000675107
- Byrne, M. E., Groover, A. T., Fontana, J. R., and Martienssen, R. A. (2003). Phylloclastic pattern and stem cell fate are determined by the Arabidopsis homeobox gene BELLRINGER. *Development* 130, 3941–3950. doi: 10.1242/dev.00620
- Caño-Delgado, A., Penfield, S., Smith, C., Catley, M., and Bevan, M. (2003). Reduced cellulose synthesis invokes lignification and defense responses in Arabidopsis thaliana. *Plant J.* 34, 351–362. doi: 10.1046/j.1365-313x.2003.01729.x
- Carland, F., and Nelson, T. (2009). CVP2-and CVL1-mediated phosphoinositide signaling as a regulator of the ARF GAP SFC/VAN3 in establishment of foliar vein patterns. *Plant J.* 59, 895–907. doi: 10.1111/j.1365-313X.2009.03920.x
- Carlsbecker, A., Lee, J.-Y., Roberts, C. J., Dettmer, J., Lehesranta, S., Zhou, J., et al. (2010). Cell signalling by microRNA165/6 directs gene dose-dependent root cell fate. *Nature* 465, 316–321. doi: 10.1038/nature08977
- Chen, Y., Li, W., Turner, J. A., and Anderson, C. T. (2021). PECTATE LYASE LIKE12 patterns the guard cell wall to coordinate turgor pressure and wall mechanics for proper stomatal function in Arabidopsis. *Plant Cell* 33, 3134–3150. doi: 10.1093/plcell/koab161
- Clough, S. J., and Bent, A. F. (1998). Floral dip: a simplified method for Agrobacterium-mediated transformation of Arabidopsis thaliana. *Plant J.* 16, 735–743. doi: 10.1046/j.1365-313x.1998.00343.x
- Domingo, C., Roberts, K., Stacey, N. J., Connerton, I., Ruiz-Teran, F., and Mccann, M. C. (1998). A pectate lyase from *Zinnia elegans* is auxin inducible. *Plant J.* 13, 17–28. doi: 10.1046/j.1365-313x.1998.00002.x
- Engler, C., Youles, M., Gruetzner, R., Ehnert, T.-M., Werner, S., Jones, J. D., et al. (2014). A golden gate modular cloning toolbox for plants. *ACS Synthet. Biol.* 3, 839–843. doi: 10.1021/sb4001504
- Etchells, J. P., Moore, L., Jiang, W. Z., Prescott, H., Capper, R., Saunders, N. J., et al. (2012). A role for BELLRINGER in cell wall development is supported by loss-of-function phenotypes. *BMC Plant Biol.* 12:212–212. doi: 10.1186/1471-2229-12-212
- Ferrari, S., Savatin, D., Sicilia, F., Gramegna, G., Cervone, F., and De Lorenzo, G. (2013). Oligogalacturonides: plant damage-associated molecular patterns and regulators of growth and development. *Front. Plant Sci.* 2013:4. doi: 10.3389/fpls.2013.00049
- Fisher, K., and Turner, S. (2007). PXY, a receptor-like kinase essential for maintaining polarity during plant vascular-tissue development. *Curr. Biol.* 17, 1061–1066. doi: 10.1016/j.cub.2007.05.049
- Furuta, K. M., Yadav, S. R., Lehesranta, S., Belevich, I., Miyashima, S., Heo, J.-O., et al. (2014). Arabidopsis NAC45/86 direct sieve element morphogenesis culminating in enucleation. *Science* 345, 933–937. doi: 10.1126/science.1253736
- Hajdukiewicz, P., Svab, Z., and Maliga, P. (1994). The small, versatile pPZP family of Agrobacterium binary vectors for plant transformation. *Plant Mole. Biol.* 25, 989–994. doi: 10.1007/BF00014672
- Hirakawa, Y., Shinohara, H., Kondo, Y., Inoue, A., Nakanomyo, I., Ogawa, M., et al. (2008). Non-cell-autonomous control of vascular stem cell fate by a CLE peptide/receptor system. *Proc. Natl. Acad. Sci.* 105:15208. doi: 10.1073/pnas.0808444105

writing—original draft. All authors: formal analysis, data curation, and writing—review and editing.

FUNDING

This work was supported by BBSRC grants BB/M003825/1, BB/S005714/1, and BBS/E/J/000PR9787.

ACKNOWLEDGMENTS

We thank the European Arabidopsis Stock Centre for seeds, G. Calder and E. Wegel for microscopy support, and members of the Sablowski laboratory past and present for helpful discussions.

SUPPLEMENTARY MATERIAL

The Supplementary Material for this article can be found online at: <https://www.frontiersin.org/articles/10.3389/fpls.2022.888201/full#supplementary-material>

- Israeli, A., Reed, J. W., and Ori, N. (2020). Genetic dissection of the auxin response network. *Nat. Plants* 6, 1082–1090. doi: 10.1038/s41477-020-0739-7
- Ito, Y., Nakanomyo, I., Motose, H., Iwamoto, K., Sawa, S., Dohmae, N., et al. (2006). Dodeca-CLE peptides as suppressors of plant stem cell differentiation. *Science* 313, 842–845. doi: 10.1126/science.1128436
- Kalmbach, L., Bourdon, M., Heo, J.-O., Otero, S., Blob, B., and Helariutta, Y. (2022). Pectin cell wall remodeling through PLL12 and callose deposition through polar CALS7 are necessary for long-distance phloem transport. *bioRxiv* 2022:478312.
- Kalmbach, L., and Helariutta, Y. (2019). Sieve plate pores in the phloem and the unknowns of their formation. *Plants* 8:25. doi: 10.3390/plants8020025
- Kondo, Y., Nurani, A. M., Saito, C., Ichihashi, Y., Saito, M., Yamazaki, K., et al. (2016). Vascular Cell Induction Culture System Using Arabidopsis Leaves (VISUAL) Reveals the Sequential Differentiation of Sieve Element-Like Cells. *Plant Cell* 28, 1250–1262. doi: 10.1105/tpc.16.00027
- Kubo, M., Udagawa, M., Nishikubo, N., Horiguchi, G., Yamaguchi, M., Ito, J., et al. (2005). Transcription switches for protoxylem and metaxylem vessel formation. *Genes Dev.* 19, 1855–1860. doi: 10.1101/gad.1331305
- Mitra, P. P., and Loqué, D. (2014). Histochemical staining of Arabidopsis thaliana secondary cell wall elements. *JoVE* 2014, e51381. doi: 10.3791/51381
- Mitsuda, N., Iwase, A., Yamamoto, H., Yoshida, M., Seki, M., Shinozaki, K., et al. (2007). NAC transcription factors, NST1 and NST3, are key regulators of the formation of secondary walls in woody tissues of Arabidopsis. *Plant Cell* 19, 270–280. doi: 10.1105/tpc.106.047043
- Miyashima, S., Roszak, P., Seville, I., Toyokura, K., Blob, B., Heo, J.-O., et al. (2019). Mobile PEAR transcription factors integrate positional cues to prime cambial growth. *Nature* 565, 490–494. doi: 10.1038/s41586-018-0839-y
- Moscattello, R., Mariani, P., Sanders, D., and Maathuis, F. J. M. (2006). Transcriptional analysis of calcium-dependent and calcium-independent signalling pathways induced by oligogalacturonides. *J. Exp. Bot.* 57, 2847–2865. doi: 10.1093/jxb/erl043
- Nieminen, K., Blomster, T., Helariutta, Y., and Mähönen, A. P. (2015). Vascular cambium development. *Arabidop. Book/Am. Soc. Plant Biol.* 2015:13.
- Peaucelle, A., Louvet, R., Johansen, J. N., Salsac, F., Morin, H., Fournet, F., et al. (2011). The transcription factor BELLRINGER modulates phyllotaxis by regulating the expression of a pectin methyltransferase in Arabidopsis. *Development* 138, 4733–4741. doi: 10.1242/dev.072496
- Rebocho, A. B., Southam, P., Kennaway, J. R., Bangham, J. A., and Coen, E. (2017). Generation of shape complexity through tissue conflict resolution. *Elife* 6:e20156. doi: 10.7554/eLife.20156
- Roeder, A. H. K., Ferrandiz, C., and Yanofsky, M. F. (2003). The role of the REPLUMLESS homeodomain protein in patterning the Arabidopsis fruit. *Curr. Biol.* 13, 1630–1635. doi: 10.1016/j.cub.2003.08.027
- Ruonala, R., Ko, D., and Helariutta, Y. (2017). Genetic networks in plant vascular development. *Annu. Rev. Genet.* 51, 335–359. doi: 10.1146/annurev-genet-120116-024525
- Schiessl, K., Kausika, S., Southam, P., Bush, M., and Sablowski, R. (2012). JAGGED controls growth anisotropy and coordination between cell size and cell cycle during plant organogenesis. *Curr. Biol.* 22, 1739–1746. doi: 10.1016/j.cub.2012.07.020
- Schindelin, J., Arganda-Carreras, I., Frise, E., Kaynig, V., Longair, M., Pietzsch, T., et al. (2012). Fiji: an open-source platform for biological-image analysis. *Nat. Methods* 9, 676–682. doi: 10.1038/nmeth.2019
- Seifert, G. J., and Blaukopf, C. (2010). Irritable Walls: the Plant Extracellular Matrix and Signaling. *Plant Physiol.* 153, 467–478. doi: 10.1104/pp.110.153940
- Sénéchal, F., Wattier, C., Rustérucci, C., and Pelloux, J. (2014). Homogalacturonan-modifying enzymes: structure, expression, and roles in plants. *J. Exp. Bot.* 65, 5125–5160. doi: 10.1093/jxb/eru272
- Serrano-Mislata, A., Schiessl, K., and Sablowski, R. (2015). Active control of cell size generates spatial detail during plant organogenesis. *Curr. Biol.* 25, 2991–2996. doi: 10.1016/j.cub.2015.10.008
- Sieburth, L. E., Drews, G. N., and Meyerowitz, E. M. (1998). Non-autonomy of AGAMOUS function in flower development: use of a Cre/loxP method for mosaic analysis in Arabidopsis. *Development* 125, 4303–4312. doi: 10.1242/dev.125.21.4303
- Sieburth, L. E., Muday, G. K., King, E. J., Benton, G., Kim, S., Metcalf, K. E., et al. (2006). SCARFACE Encodes an ARF-GAP That Is Required for Normal Auxin Efflux and Vein Patterning in Arabidopsis. *Plant Cell* 18, 1396–1411. doi: 10.1105/tpc.105.039008
- Smit, M. E., McGregor, S. R., Sun, H., Gough, C., Bågman, A.-M., Soyars, C. L., et al. (2020). A PXY-mediated transcriptional network integrates signaling mechanisms to control vascular development in Arabidopsis. *Plant Cell* 32, 319–335. doi: 10.1105/tpc.19.00562
- Smith, H. M. S., and Hake, S. (2003). The interaction of two homeobox genes, BREVIPEDICELLUS and PENNYWISE, regulates internode patterning in the Arabidopsis inflorescence. *Plant Cell* 15, 1717–1727. doi: 10.1105/tpc.012856
- Smyth, D. R., Bowman, J. L., and Meyerowitz, E. M. (1990). Early flower development in Arabidopsis. *Plant Cell* 2, 755–767. doi: 10.2307/3869174
- Speer, E. (1987). A method of retaining phloroglucinol proof of lignin. *Stain Technol.* 62, 279–280. doi: 10.3109/10520298709108008
- Sugiyama, Y., Wakazaki, M., Toyooka, K., Fukuda, H., and Oda, Y. (2017). A Novel Plasma Membrane-Anchored Protein Regulates Xylem Cell-Wall Deposition through Microtubule-Dependent Lateral Inhibition of Rho GTPase Domains. *Curr. Biol.* 27, 2522.e–2528.e. doi: 10.1016/j.cub.2017.06.059
- Sun, H., Hao, P., Gu, L., Cheng, S., Wang, H., Wu, A., et al. (2020). Pectate lyase-like Gene GhPEL76 regulates organ elongation in Arabidopsis and fiber elongation in cotton. *Plant Sci.* 293:110395. doi: 10.1016/j.plantsci.2019.110395
- Sun, L., and Van Nocker, S. (2010). Analysis of promoter activity of members of the PECTATE LYASE-LIKE (PLL) gene family in cell separation in Arabidopsis. *BMC Plant Biol.* 10, 1–13. doi: 10.1186/1471-2229-10-152
- Uluisk, S., and Seymour, G. B. (2020). Pectate lyases: their role in plants and importance in fruit ripening. *Food Chem.* 309:125559. doi: 10.1016/j.foodchem.2019.125559
- Wang, Y., Wang, J., Shi, B., Yu, T., Qi, J., Meyerowitz, E. M., et al. (2014). The Stem Cell Niche in Leaf Axils Is Established by Auxin and Cytokinin in Arabidopsis. *Plant Cell* 26, 2055–2067. doi: 10.1105/tpc.114.123083
- Wolf, S., Hématy, K., and Höfte, H. (2012). Growth control and cell wall signaling in plants. *Annu. Plant Biol.* 63, 381–407. doi: 10.1146/annurev-arplant-042811-105449
- Yang, Y., Yu, Y., Liang, Y., Anderson, C. T., and Cao, J. (2018). A Profusion of Molecular Scissors for Pectins: classification, Expression, and Functions of Plant Polygalacturonases. *Front. Plant Sci.* 2018:9. doi: 10.3389/fpls.2018.01208
- Zhong, R., Lee, C., Haghghat, M., and Ye, Z.-H. (2021). Xylem vessel-specific SND5 and its homologs regulate secondary wall biosynthesis through activating secondary wall NAC binding elements. *New Phytol.* 231, 1496–1509. doi: 10.1111/nph.17425

Conflict of Interest: The authors declare that the research was conducted in the absence of any commercial or financial relationships that could be construed as a potential conflict of interest.

Publisher's Note: All claims expressed in this article are solely those of the authors and do not necessarily represent those of their affiliated organizations, or those of the publisher, the editors and the reviewers. Any product that may be evaluated in this article, or claim that may be made by its manufacturer, is not guaranteed or endorsed by the publisher.

Copyright © 2022 Bush, Sethi and Sablowski. This is an open-access article distributed under the terms of the Creative Commons Attribution License (CC BY). The use, distribution or reproduction in other forums is permitted, provided the original author(s) and the copyright owner(s) are credited and that the original publication in this journal is cited, in accordance with accepted academic practice. No use, distribution or reproduction is permitted which does not comply with these terms.